**Proceedings of SAMPE 2007. Baltimore, MD. 3-7 June 2007.**

# MULTI-THREAT PERFORMANCE OF KAOLIN-BASED SHEAR THICKENING FLUID (STF)-TREATED FABRICS

Brian A. Rosen[1], Caroline H. Nam Laufer[1], Dennis P. Kalman[1], Eric D. Wetzel[2], and Norman J. Wagner[1]

[1]Department of Chemical Engineering at the University of Delaware, Newark DE 19716
[2]U.S. Army Research Laboratory, Aberdeen Proving Ground, MD 21005

KEYWORDS: Armor Technology, Aramid Fiber Composites, Materials-Clay

## ABSTRACT

The goal of this research is to investigate the shear-thickening of highly loaded kaolin clay suspensions for use in protective fabrics. The nominal 500 nm diameter kaolin clay platelets are similar in size but different geometrically than the spherical silica particles used in previous STF formulations. Rheological measurements show that a dispersion of kaolin particles suspended in glycerol ($\Phi = 0.43$) begins to continuously shear thicken at a shear stress of 12 Pa. Upon intercalating the STF into Kevlar®, the composite STF-Kevlar shows a marked increase in spike and needle resistance, as well as a reduction in yarn pullout. Quasi-static stab tests on four layers of Kevlar impregnated with the kaolin STF show that the sample can prevent penetration of an NIJ standard spike at loads up to 160 N. The same four layers of neat Kevlar are penetrated at just 35 N. Finally, the $V_{50}$ velocity of single-layer STF-treated Kevlar fabric, using 0.22 caliber spherical steel projectiles, was found to be ~ 50% higher than that of neat Kevlar fabric and similar to the standard STF-Kevlar composite. We find evidence that the platelet particle STFs may provide additional protective benefits as compared with spherical particle STFs as the size of the threat decreases. The results of this research can aid in the development of a broad range of protective materials for both consumer and military applications.

## 1. INTRODUCTION

High performance woven fabrics composed of materials such as Kevlar® are used in many protective applications, including both ballistic and stab body armors. There are many cooperative mechanisms that collectively describe how these woven fabrics disperse the energy from a projectile or stab threat. These mechanisms include yarn rotation, lateral sliding, uncrimping, translation, plastic deformation and fracture (Cheeseman et al., 2003). The stab and ballistic resistance of neat fabrics has been shown to increase upon impregnation with shear thickening fluids (STFs) (Lee et al., 2003). STFs are colloidal suspensions of solid particles in a liquid carrier. At high volume fractions, high shear stresses cause the suspended colloidal particles to form hydroclusters. Hydrocluster formation leads to a viscosity increase that can, at sufficiently high particle loading, result in a solid-like response, which is termed discontinuous shear thickening. Previous work (Lee et al., 2003) has shown that a suspension of 450 nm silica particles in poly (ethylene glycol) will discontinuously shear thicken at volume fractions of about 0.52.

STFs can be formulated using a wide range of solid particulate and liquid components. In theory, it may be possible to tailor the STF to a specific threat by changing the size, shape, or composition of the particle (Wetzel et al., 2004). Most existing studies on STF-fabrics have focused on spherical or rod-like silica particles (Egres 2005). Spherical particles, however, do not allow for the most efficient packing, limiting their ultimate volume fraction loading in the STF. In addition, they may not be the most efficient geometry for distributing stresses from a force point source. For example, oblate ellipsoids or plate-like particles may be more efficient at laterally dispersing energy or distributing stresses due to alignment or stacking effects, which could be beneficial in imparting ballistic and stab resistance. Testing this conjecture is one aim of this study.

One candidate, non-spherical particle is kaolin clay, which has a platelet particle shape and has been shown to form shear thickening dispersions. Commercial kaolin clay particles have been shown to continuously shear thicken when suspended in water at 70 wt% (Egres, 2005). Kaolin particles are commercially available at relatively low cost as compared to the monodisperse silica particles used previously, which is also advantageous for their application in protective materials. Here, we disperse Kaolin in glycerol, a less volatile solvent than water, which enables the formulation of STF treated fabrics for possible use as ballistic and stab resistant materials. In the following, suspensions of Kaolin in glycerol are denoted as K-STF to distinguish them from the spherical particle STF (S-STF).

This study compares the rheology and performance of fabrics treated with K-STF to fabrics treated with S-STF composed of spherical silica. Quasi-static and ballistic tests are performed. Quasi-static tests measure the load and energy absorbed by fabrics from very low speed cut and puncture threats. Ballistic testing assesses the penetration resistance of fabrics against higher velocity impacts.

## 2. EXPERIMENTAL

**2.1 Materials** All targets are based on scoured Hexcel-Schwebel style 706 woven Kevlar fabric (600 denier KM2, 34 × 34 ypi), with an areal density of 180 g/m$^2$. The dry kaolin clay particles, supplied by the Engelhard Corporation (Iselin, NJ), have a mean size of 500 nm with 12-22 percent of the particles above 2 microns. The particle density is 2.58 g/cc and the bulk powder contains less than 1% moisture as indicated by the manufacturer. Figure 1 shows SEM images of the kaolin clay particles. The SEM images illustrate the shape and relative polydispersity of the dry kaolin clay particles. Although the particles are not monodisperse, the focus of this research is to evaluate the ability of flat clay particles in bulk to enhance the performance of neat Kevlar.

The K-STF was synthesized by mixing dry kaolin particles with glycerol (Fischer) using a Waring Commercial Heavy Duty Blender. In order to stay within the capacity of the blender, the STF was synthesized in steps. First, the full volume of glycerol was added to the blender. Afterwards, 35% of the total weight of kaolin particles was added to the blender and mixed with the glycerol for 1 minute at the “low” blender setting (11,000 rpm). Then, an additional 35% of the total weight of kaolin was added and again mixed at the same speed for one minute. Finally, the remainder of the clay was added and allowed to mix for 1 min using the “medium” setting. It was shown in this study that the processing parameters such as the blending time and speed did not affect the overall rheology of the fluid.

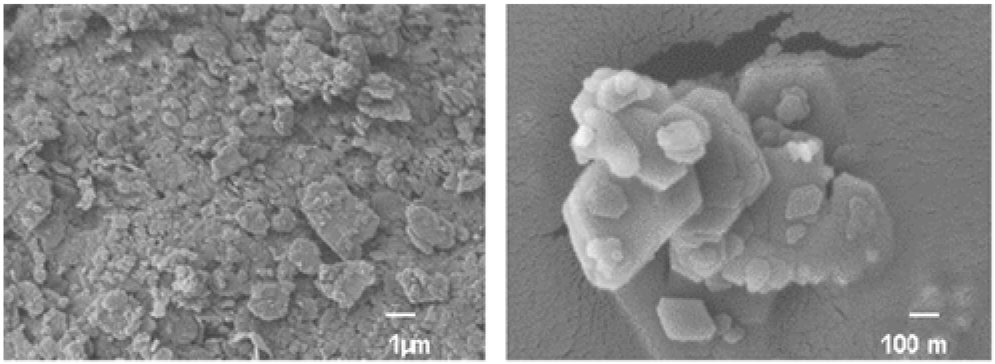


**Figure 1: SEM images of dry kaolin particles (avg. size 500nm).**

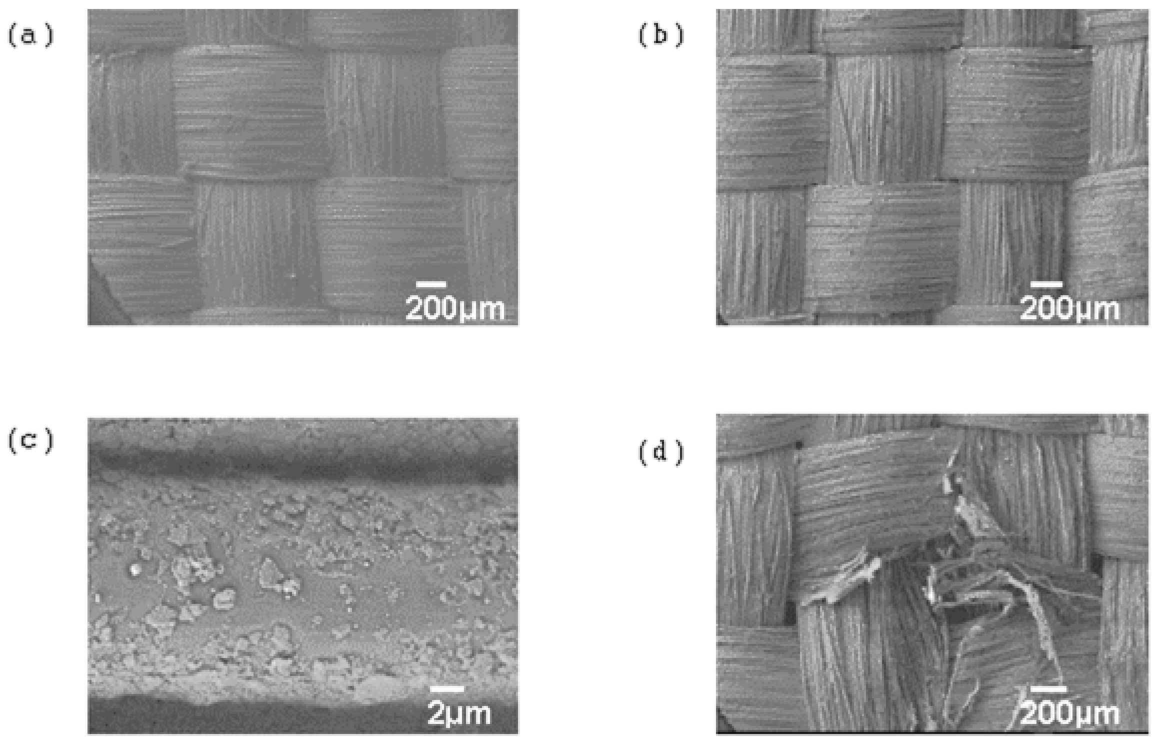


**Figure 2: (a) Neat Kevlar, (b, c) Kevlar impregnated with the K-STF, and (d) K-STF Kevlar after quasi-static spike test.**

In order to intercalate the K-STF into the Kevlar, the K-STF was diluted at a volume ratio of 3:1 absolute ethanol (Fischer) to STF. Each 38.2-cm × 38.1-cm piece of Kevlar was submerged in the dilute ethanol-STF mixture for 1 minute. While the Kevlar was in solution, a cover was placed over the container to minimize ethanol evaporation. Once the first minute expired, the Kevlar piece was flipped and submerged for another minute. After the second minute, the Kevlar was squeezed through rubber-coated nip rollers two times in order to remove the excess fluid. The samples were allowed to air dry for approximately 10 minutes, after which they were placed in an industrial oven at 80°C for 30 minutes to allow all of the ethanol to evaporate. Repeating this process for a second coating of K-STF was required to set the 18% wt addition to the fabric used throughout this study. Figure 2a shows an SEM image of untreated fabric, while Figs. 2b-c show the K-STF-treated fabric. The clay appears to be evenly dispersed throughout the fabric, and has effectively intercalated the fabric to coat individual Kevlar filaments.

For comparison, additional STF-fabrics based on 450 nm spherical silica were also prepared according to previously published methods (Lee, 2003). Stab and ballistic characterizations were performed on neat, K-STF-treated, and spherical STF-treated fabrics with areal densities of 210 and 216 g/m$^2$ respectively. We use the notation "S-STF-706" to refer to targets treated with the spherical particle based STF.

**2.2 Rheology** The kaolin suspensions were characterized using an AR G-2 stress-controlled rheometer manufactured by TA Instruments. The tool geometry used was a 20 mm 2º cone and Peltier plate set at 25ºC. The sample was pre-sheared for 1 minute at 0.1 Pa and then examined with multiple, sequential steady-state stress sweeps. These sweeps ranged from 0.1 to 2000 Pa in the ascending direction and 2000 to 0.1 Pa in the descending direction. In order to prevent the sample from drying during long runs, a solvent trap was used. In order to minimize moisture effects, silicone oil was placed at the interface of the solvent trap and the Peltier plate.

**2.3 Quasi-static Stab Test** An Instron Model 4201 load frame, equipped with a 1 kN load cell, was used to perform the quasi-static stab tests. Tests were performed by mounting a penetrator into the crosshead of the load frame, and then displacing the penetrator into a fabric target at the rate of 5 mm/min. The targets were backed by a multi-layer foam backing, based on the National Institute of Justice (NIJ) standard 0115.0. This backing consists of four layers of 5 mm-thick neoprene sponge, followed by one layer of 31-mm-thick polyethylene foam (Houghton, 2007). All quasi-static testing was conducted on four-layer targets.

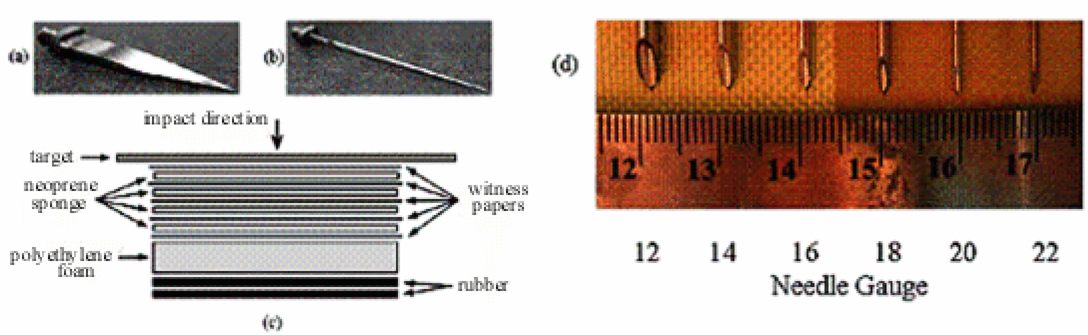


**Figure 3: (a) NIJ knife, (b) NIJ spike, (c) schematic of the foam backing used in the quasi-static stab tests, and (d) hypodermic needles.**

Quasi-static testing of the targets was conducted using three different threats: NIJ knife (type S1), NIJ spike, and stainless steel Sharpvet hypodermic needles. Four different hypodermic needle sizes were used, 12, 16, 18, and 22, corresponding to outside diameters of 2.77, 1.65, 1.27, and 0.71 mm, respectively. Testing was repeated 5 times for each threat and showed reproducibility with minimal variance of data. For each condition, data shown in this report are results from one of these five repetitions. Figure 3 shows an image of the knife, spike, and hypodermic needles, and the foam backing. Much like the NIJ spike, the hypodermic needle impacts the fabric at one point; however, like the NIJ knife, the hypodermic needle also has a cutting edge along its tip (Houghton et al., 2007). During quasi-static testing, most penetrators were displaced a total of 20 mm past the initial point of contact with the target. One exception is the 22-gauge needle, whose shaft is shorter than 20 mm and so was only displaced to a total of 10 mm.

Load versus displacement is recorded for each target and penetrator. Higher loads indicate higher resistance to penetration.

**2.4 $V_{50}$ Ballistic Test** Ballistics testing on the STF-Kevlar composites was conducted using a smooth-bore, helium pressurized gas gun. Spherical steel projectiles of 0.22 caliber and ~ 0.62 g were used. Two parallel, light-triggered chronographs were used to measure time-of-flight for calculation of impact velocities.

Single layer, 5.1 cm × 19.1 cm fabric samples were prepared and stapled to wooden blocks. These blocks were then lightly tensioned and mounted on a wooden frame (Figure 4). Behind the target was a polyethylene bag that acted as a witness. Each target was impacted one time, at the center of the target. The impact velocity was varied to induce a mixture of partial and complete penetrations. Complete penetrations are defined as impacts that cause the projectile to fall into the witness bag, or penetrate through the witness bag. All other impacts are considered partial penetrations. The $V_{50}$ velocity of a fabric is the velocity at which the projectile has a 50% chance of penetrating through the target. This $V_{50}$ was calculated by taking the five highest velocity partials and five lowest velocity completes (N=10) and averaging these ten velocities.

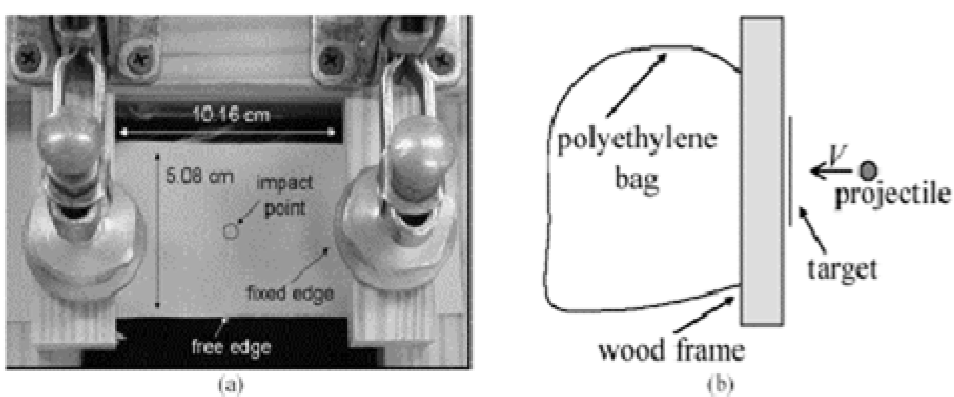


**Figure 4: Photograph and schematic diagram of helium gun target.**

# 3. RESULTS AND DISCUSSION

**3.1 Rheology** Figure 5 summarizes the steady-state rheology of K-STF ($\Phi = 0.43$) showing the viscosity of the fluid as a function of shear rate and shear stress. The shear rate at which the suspension begins to shear thicken is approximately 0.1 $s^{-1}$. The slope of the linear portion of the shear thickening region (in the $\eta$ vs. $\sigma$ plot) is 0.70, making K-STF a continuously shear thickening fluid. Note that a discontinuously shear thickening fluid would generate a slope greater than or equal to 1. Both the critical shear rate and the slope remain relatively constant over multiple (30+) stress sweeps and hysteresis was minimal. In addition, the viscosity of K-STF increases by an order of magnitude over a relatively small range of shear.

## 3.2 Stab and Ballistic Performance

***3.2.1 Quasi-static Spike Resistance*** Figure 6 compares the quasi-static spike performance of the K-STF-706, S-STF-706, and neat 706 targets. The STF and K-STF curves are the same up to approximately 7 mm of displacement, at which point the STF target is able to resist the spike penetration more that the K-STF target. At the maximum displacement of 20 mm, the difference between the K-STF and S-STF target loads is about 20 N.

Figures 2b and 2d show the K-STF fabric target before and after spike testing. The spike-tested sample shows local damage, including fiber fracture and perhaps flattening of filaments. There is some evidence of limited yarn motion. These damage modes are consistent with earlier observations of spike loading into STF-treated fabrics (Decker et al., 2007).

***3.2.2 Quasi-static Knife Resistance*** In the spike test, the fabric only needs to prevent the penetration of the tip of the spike. In contrast, during knife testing the fabric must resist both the tip and the cutting edge of the knife. Figure 7 shows the force versus displacement curves for the quasi-static knife test. The plot shows that the K-STF fabric outperforms the neat fabric. This result is consistent with previous studies, which showed that STF treatment can increase the knife resistance of Kevlar fabrics (Decker, 2007). K-STF and S-STF- fabrics perform similarly.

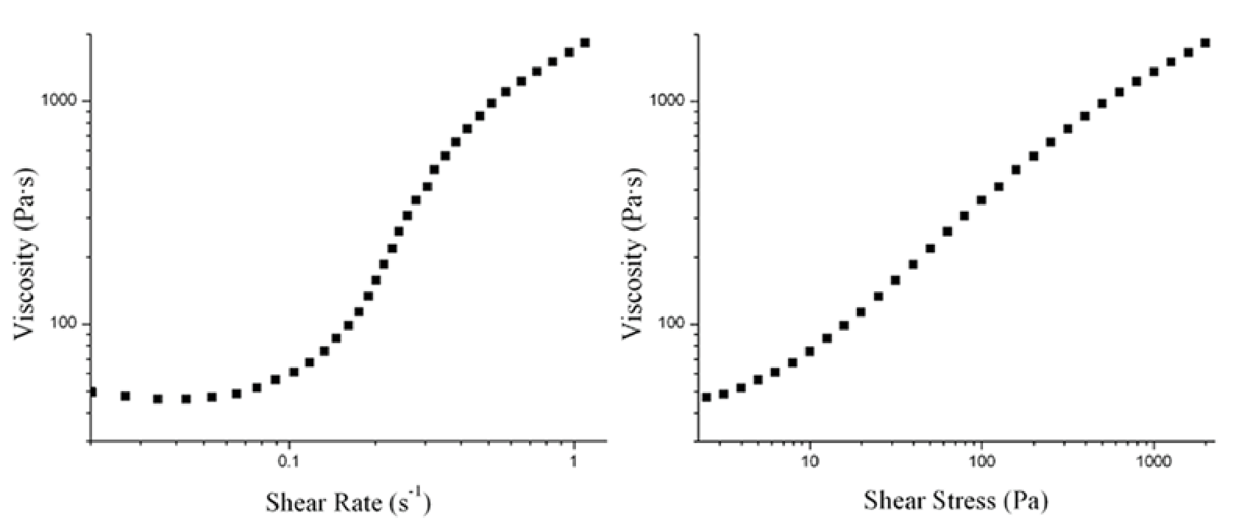


**Figure 5: Rheology of K-STF.**

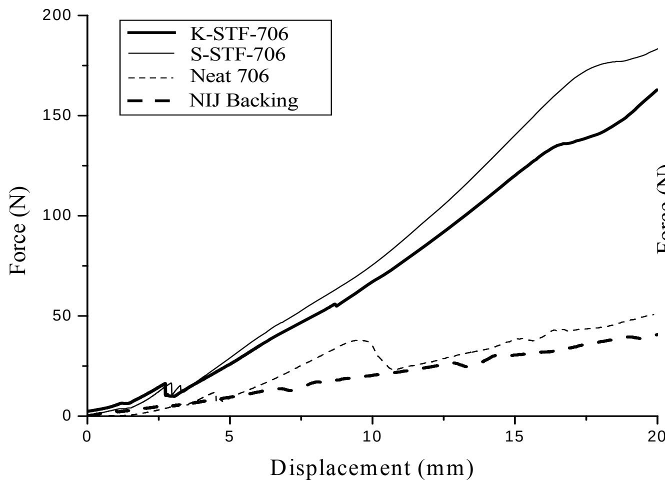


**Figure 6: Quasi-static spike test results.**

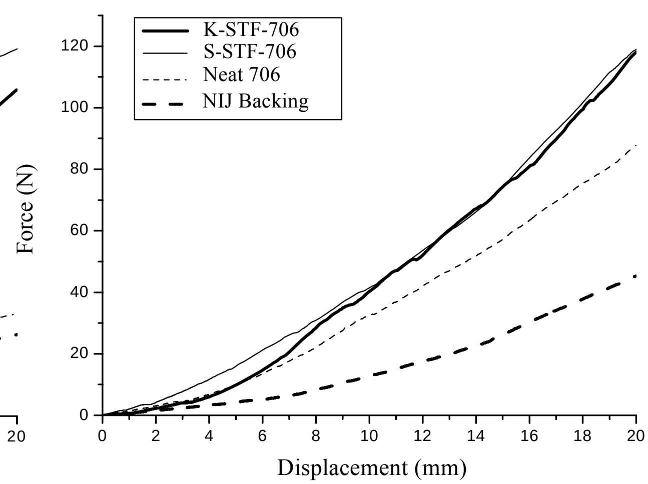


**Figure 7: Quasi-static knife test results.**

***3.2.3 Quasi-static Needle Resistance*** Figure 8 shows the displacement vs. load for the fabric targets under quasi-static loading by hypodermic needles. For both the 12 and 16 gauge needles, the K-STF and S-STF samples perform similarly up to approximately 5 mm displacement. In the case of the 12-gauge needle, the STF is able to withstand the needle to the full 20 mm whereas the K-STF composite reached a first peak load at approximately 14 mm. As the needle size is decreased to 16, 18, and 22-gauge, the K-STF fabric and S-STF fabric perform similarly.

The energy absorbed during needle puncture can be calculated by integrating the force versus displacement curves, and then subtracting the contributions from the foam backing. Calculations are performed out to 20 mm displacement for all gauges except for the 22-gauge, where the maximum displacement is 10 mm. The foam backing energy contributions are measured by performing quasi-static needle penetrations into the foam backing alone, without a target. Figure 9 shows the resulting energy absorption values as a function of needle size. The data reported are results from one of the five repetitions of the tests. The K-STF and S-STF targets show consistently higher energy absorption than the untreated target. For the largest, 12 gauge needle, the S-STF target shows slightly higher energy absorption than the K-STF sample. However, for the three smaller needle sizes, the K-STF target shows slightly higher energy absorption. These results could indicate that the flat shape of the kaolin particles provide some protective advantage over spherical particles. More data is required to confirm this trend. Note that, although the tip of the needle is larger than the surface area of a single kaolin particle, hydroclusters of clay particles might become comparable to the size of the needle tip.

Table 1 summarizes the performance results for the fabrics of interest in this study.

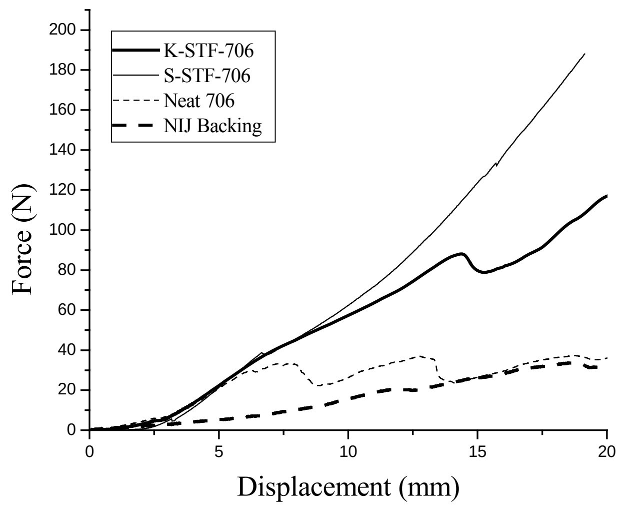


**(a)**

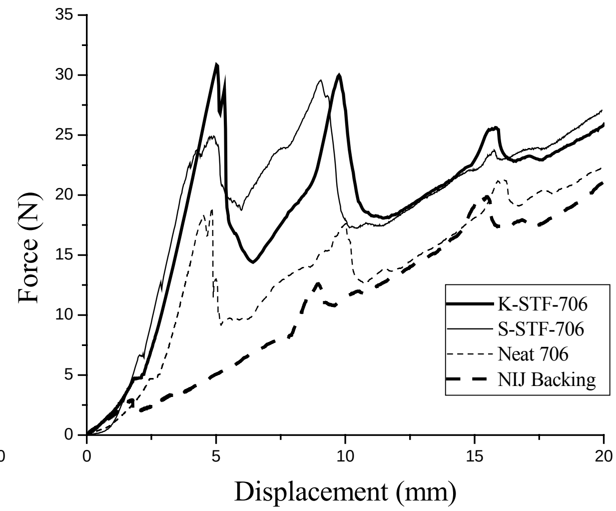


**(b)**

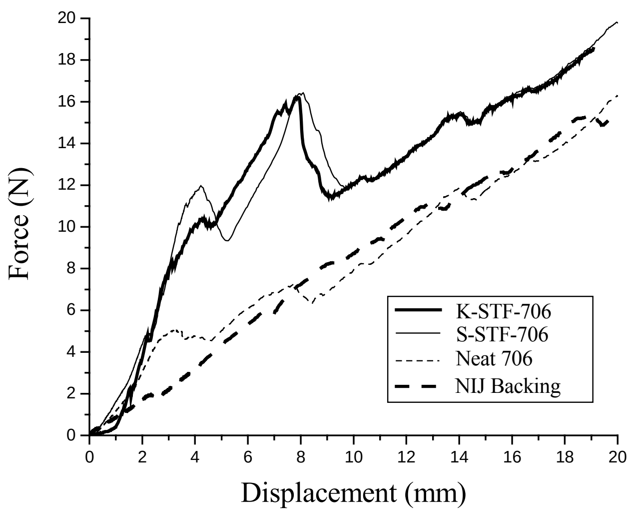


**(c)**

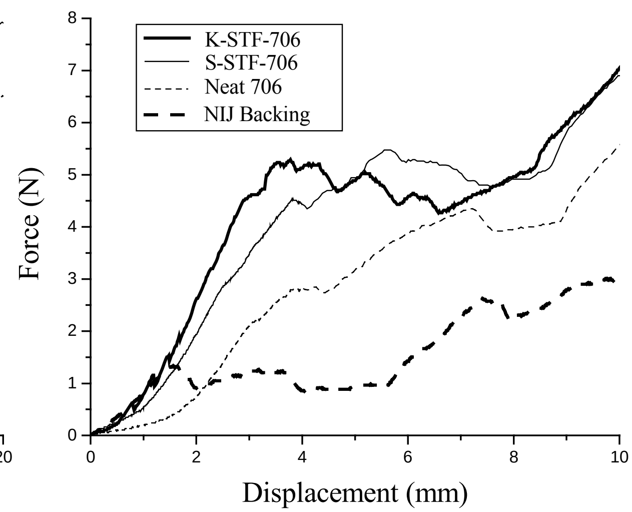


**(d)**

**Figure 8: Quasi-static needle test results for (a) 12-gauge, (b) 16-gauge, (c) 18-gauge, and (d) 22-gauge needles.**

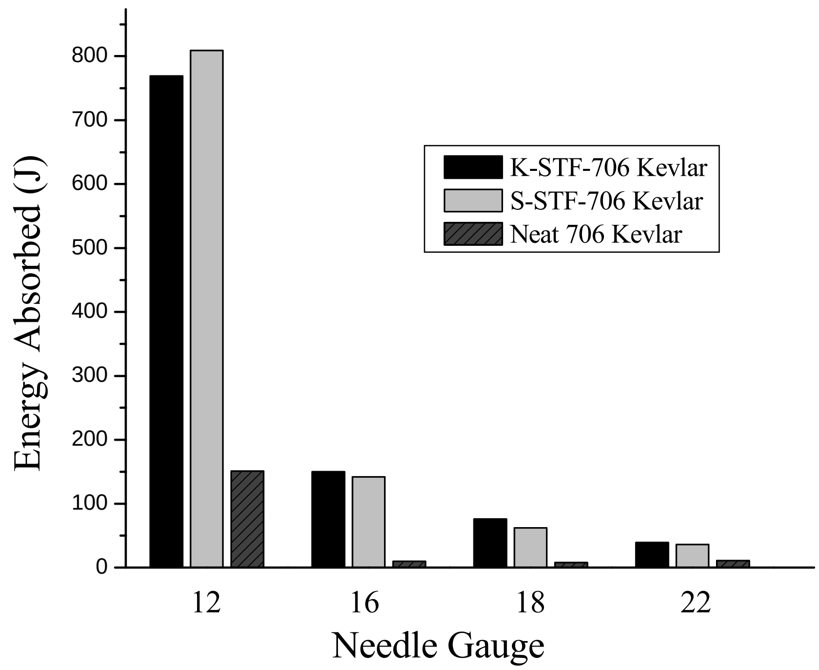


**Figure 9: Energy absorbed during quasi-static needle puncture.**

**Table 1: Overall performance comparisons between neat 706 Kevlar, K-STF-706 and S-STF-706.**

| Metric | Units | 706 | Material<br>K-STF-706 | S-STF-706 |
|---|---|---|---|---|
| Areal density (per layer) | (g/m$^2$) | 180 | 210 | 216 |
| Quasi-static loads at 20 mm | | | | |
| Spike | (N) | 35 | 160 | 180 |
| Knife | (N) | 80 | 120 | 120 |
| Energy absorbed | | | | |
| 12 gauge HN | (J) | 150 | 760 | 810 |
| 16 gauge HN | (J) | 9 | 155 | 150 |
| 18 gauge HN | (J) | 8 | 76 | 62 |
| 22 gauge HN | (J) | 11 | 39 | 36 |
| $V_{50}$ | (m/s) | 100 | 150 | 250 |

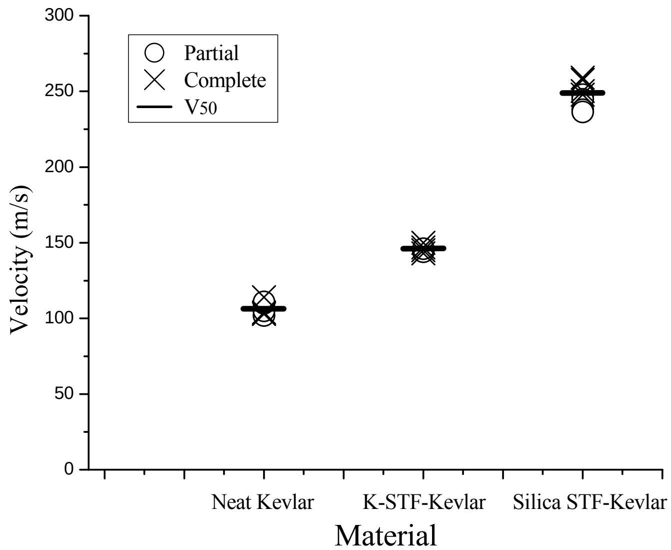


**Figure 10: $V_{50}$ data for 1 layer of neat, K-STF and S-STF fabrics.**

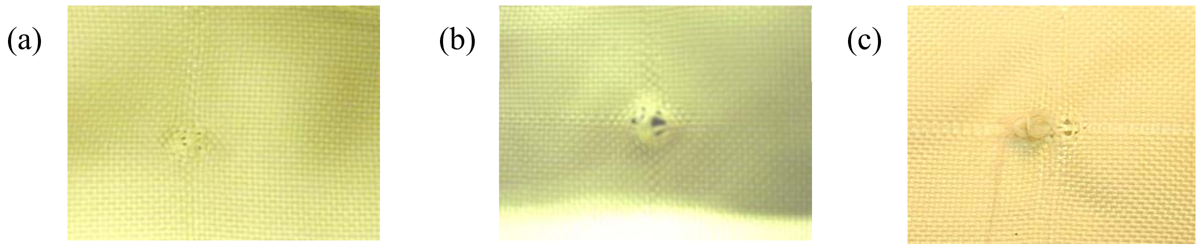


**Figure 11: K-STF composite samples after ballistic testing. (a) Partial penetration at 144m/s, (b) partial penetration at 147m/s, and (c) complete penetration at 150m/s**.

***3.2.4 Ballistic Performance*** Figure 10 shows the $V_{50}$ data for the single-layer fabric targets. The K-STF $V_{50}$ is higher than that of the neat fabric, and the S-STF $V_{50}$ is higher than both the K-STF and neat targets.

Figure 11 shows targets after ballistic impact. At speeds around or below 144 m/s (Figure 11a), the K-STF intercalated Kevlar defeats the projectile and only minimal damage is observed. Note that at this speed, the projectile would have penetrated neat Kevlar. At higher velocities (Figure 11b) the projectile is still stopped, but the yarns undergo large relative displacements without significant fracture. Finally, at velocities above 150 m/s, significant fiber fracture occurs and the projectile penetrates the fabric. Similar damage mechanisms for fabric targets impacted at low velocity have been discussed previously (Kirkwood et al., 2004).

## 4. CONCLUSIONS

In order to evaluate the effect of particle shape on STF-fabric performance, comparisons were made between the neat fabric, a clay-based K-STF fabric, and a standard, spherical particle S-STF fabric. The K-STF exhibits continuous shear thickening whereas the S-STF exhibits a discontinuous shear-thickening response. In a K-STF treated Kevlar fabric, the K-STF is dispersed evenly throughout the fibers and appears to coat the Kevlar tows with reasonable uniformity. Over a range of quasi-static stab experiments, the K-STF fabrics perform comparably to S-STF fabrics, and both perform better than untreated fabric. For small diameter hypodermic needles (12-gauge), the flat particle K-STF slightly outperforms the spherical silica particle S-STF. This increase in performance may be due to the shape or aspect ratio of the particle. Under ballistic testing, the K-STF fabrics performed better than neat fabric, but poorer than S-STF fabrics. Because K-STF performs comparably to the S-STF in defeating stab and puncture threats, clay-based STF-fabrics may be a viable alternative to silica-based STF-fabrics. The raw materials for K-STFs are readily available, which could potentially make clay-based STFs more economical for some applications.

## 5. ACKNOWLEDGEMENTS

Research was sponsored by the U.S. Army Research Office and U.S. Army Research laboratory and was accomplished under Cooperative Agreement Number W911NF-05-2-0006. The views and conclusions contained in this document are those of the authors and should not be interpreted as representing the official policies, either expressed or implied, of the Army Research office, Army Research Laboratory, or the U.S. Government. The U.S. Government is authorized to reproduce and distribute reprints for Government purposes notwithstanding any copyright notation hereon.

## 6. REFERENCES

B.A. Cheeseman and T.A. Bogetti, Comp. Struct., 61, 161 (2003).

M.J. Decker, C.J. Halbach, C.H. Nam, N.J. Wagner, and E.D. Wetzel, Composites Science and Technology, 67 (3-4), 565 (2007).

R.G. Egres, PhD Dissertation, University of Delaware (2005).

J. Houghton, B. Schiffman, D. Kalman, E.D. Wetzel, and N.J. Wagner, Proceedings, SAMPE 2007, Baltimore, MD.

J.E. Kirkwood, K.M. Kirkwood, Y.S. Lee, R.G. Egres, E.D. Wetzel, and N.J. Wagner, Textile Research Journal, 74 (11), 939 (2004).

K.M. Kirkwood, J.E. Kirkwood, E.D. Wetzel, Y.S. Lee, and N.J. Wagner, Textile Research Journal, 74 (10), 920 (2004).

Y.S. Lee, E.D. Wetzel, and N.J. Wagner, J. Mat. Sci., 38 (13), 2825 (2003).

E.D. Wetzel, Y.S. Lee, R.G. Egres, K.M. Kirkwood, J.E. Kirkwood, and N.J. Wagner, Proceedings, NUMIFORM 2004, Columbus, OH.